

ABOVEGROUND BIOMASS AND CARBON STOCK ESTIMATION OF FALCATA THROUGH THE SYNERGISTIC USE OF SENTINEL-1 AND SENTINEL-2 IMAGES

J. L. E. Gesta ^{1,2}, J. M. Fernandez ¹, R. S. Lina ¹, J. R. Santillan ^{1,2}

¹ Department of Geodetic Engineering, College of Engineering and Geosciences, Caraga State University, Ampayon, Butuan City, 8600, Philippines

² Caraga Center for Geo-Informatics, Caraga State University, Ampayon, Butuan City, 8600, Philippines
(jrsantillan, jlegesta, rosalia.lina, joyjoy.fernandez)@carsu.edu.ph

Commission IV, WG7

KEY WORDS: Aboveground Biomass, Carbon Content, Allometric Equation, *Paraserianthes falcata* (L.) Nielson, Remote Sensing

ABSTRACT:

Estimates of aboveground biomass (AGB) in forests have been made in the context of climate change mitigation. There were limited studies about Falcata aboveground biomass and carbon stock estimation using the traditional method; however, that is time-intensive and expensive. Hence, this study was executed to utilize remote sensing and assess the potential of the synergistic use of Sentinel-1 and Sentinel-2 images in estimating the AGB and carbon stock of Falcata. The methodology consists of boundary demarcation of Falcata plantations in Butuan City, development of aboveground biomass models, and estimation and mapping of aboveground biomass and carbon stock. Among the developed models, the model which is the combination of Sentinel-1 and Sentinel-2 has the highest coefficient of determination (R^2) of 0.632 and lowest Root Mean Square Error (RMSE) of 1.94 ton/pixel and was found to perform best in predicting the AGB and carbon stock of 4-year-old Falcata and performed poorly in 1-year-old Falcata. Nevertheless, its overall R^2 and RMSE have proven that the model is moderately good and acceptable in predicting AGB of all stand ages of Falcata and, indirectly, the carbon stock. This study demonstrates that combining satellites generates a robust and more accurate AGB and Carbon Stock model than the models derived from the individual satellites.

1. INTRODUCTION

Climate change and its manifestations, notably increased temperatures, changing precipitation patterns, and rising sea levels, are worldwide environmental concerns that can impact many countries' ecological and socioeconomic systems (IPCC, 1996). Tropical rainforests, in particular, significantly contribute to the global carbon cycle by storing approximately 40% of the world's terrestrial carbon (Maurya et al., 2015). Since forests store more carbon dioxide than the entire atmosphere, their role is critical (Stern, 2006). Like other tropical forests, Philippine forests have the highest potential for carbon sequestration, mainly through the development of forest plantations and the conservation of existing forests as carbon sinks (Lantican, 2020). The Falcata is one of the fastest-growing species in the Philippines. It is classified as an Industrial Tree Plantation Species (ITPs), and this species is commonly utilized in forest plantations, reforestation, and agroforestry (Chauhan et al., 2019). Quantifying aboveground biomass (AGB) is one of the indicators of carbon storage and sequestration of forests (Bolastig, 2019). Moreover, carbon stock estimation is critical in determining the extent of carbon exchange between the forest ecosystem and the atmosphere (Vashum, 2012).

Biomass calculated from field data measurement is the most reliable, but it is not a realistic approach for large-scale assessments. Remote Sensing takes hold because it can provide data over a large area for a fraction of the cost of extensive sampling and allows access to previously inaccessible areas. Remote sensing satellite data is available at various scales, from local to global and on various platforms. There are also different kinds of data, such as optical, radar, and LiDAR, each with advantages (Steiner et al., 2022).

The European Space Agency's (ESA) Sentinel satellite constellation series, including the Sentinel-1 C-band Synthetic Aperture Radar (SAR) and the Sentinel-2 multispectral instrument, provides advanced capabilities for AGB mapping with extensive coverage, a short return cycle, and a long lifespan as the same data format (Powell et al., 2010). Although remotely sensed optical images were used in several experiments, the biomass values extracted from optical data can saturate quickly, particularly in densely vegetated areas. As an alternative, Synthetic Aperture Radar (SAR) has been proposed, claiming that it can counter the disadvantages of optical sensors. Based on the shortcomings and benefits of optical and SAR sensors, recent attempts have been made to incorporate the complementary knowledge contained in these two data sources concerning land cover applications (Nuthammachot et al., 2020).

Estimates of aboveground biomass and carbon stock of Falcata Plantations are imperative to the context of forest inventory and climate change mitigation. There were limited studies of Falcata AGB and carbon stock and utilized only the traditional approach, which is costly and time extensive. Currently, there is no study about AGB and carbon stock estimation of Falcata plantation using the remote sensing approach. This paper introduced and proved the capability of utilizing satellite images, particularly Sentinel-1 and Sentinel-2 images, in estimating AGB and Carbon Stock of Falcata Plantations in Butuan City.

2. METHODOLOGY

2.1 Study Area

The study was conducted in Butuan City, Agusan del Norte, Philippines (Figure 1). It has a land area of 81,662 hectares, roughly 4.1% of the total area of the Caraga region. It has total forestland of 272.5 square kilometers, wherein 38.5% of it is

production forest areas mainly grown with industrial tree species, one of which is Falcata Plantations. The dominant Falcata species found in the area is the *Paraserianthes falcataria* (L.) Nielson (Krisnawati et al., 2011).

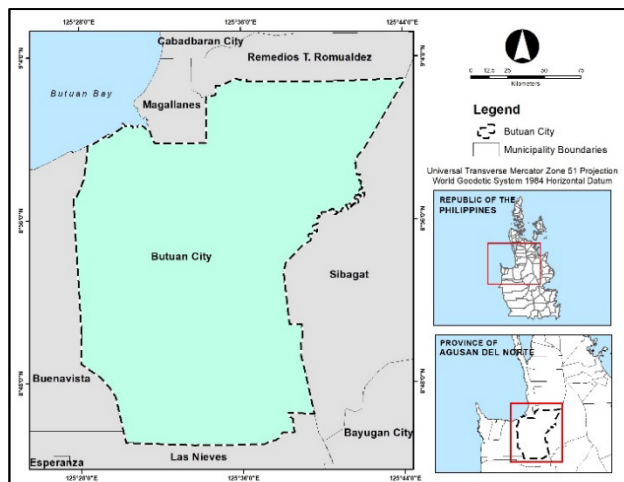


Figure 1. Map of the Study Area.

2.2 Boundary Demarcation of Falcata Plantations

Sentinel-2 image at level-2A, acquired on July 23, 2021, was utilized for boundary demarcation of Falcata plantations since it has less cloud cover in Butuan City. The satellite image was then used for image classification using Random Forest classifier, and the classified image was subjected to accuracy assessment. The final classified image, which is cloud-free, was then refined using Google Earth to correct most of the misclassified pixels of Falcata. The refined classified image was then used to extract the Falcata boundaries of Falcata plantations in Butuan City.

2.3 Model Development

2.3.1 Field Data Collection. The field data were collected from Falcata plantations in the study area, which was conducted on November 6 to 12, 2021. The diameter-at-breast height (DBH) and tree height of Falcata inside the plots were measured. Also, the corner geographic coordinates of the plots were recorded, which were used to locate the center coordinates accurately. A total of fifty-six (56) plots were established randomly. Representative plots for Falcata ages 1 to 8 were established. There are six plots for 1-year-old Falcata, eight for 2-year-old Falcata, and seven for 3- to 8-year-old Falcata. There were fewer plantations for 1-year-old Falcata, which made the number of representative plots not the same. For the development of the aboveground biomass model, forty (40) plots were randomly assigned, four plots for 1-year-old Falcata, six plots for 2-year-old Falcata, and five plots each for 3- to 8-year-old Falcata. The remaining sixteen (16) plots were assigned for accuracy assessment or validation of the model, consisting of 2 plots for each year of Falcata.

2.3.2 Satellite Data Acquisition and Pre-processing. The Sentinel-1B image taken on July 25, 2021, was acquired from European Space Agency's (ESA) Data Hub and pre-processed on SNAP Software. The images underwent four phases: orbit file, radiometric calibration, speckle filtering, and geometric correction. The image was spatially resampled from 10-meter to 20-meter pixel resolution to approximate the size of the field plots and the Sentinel-2 image. The grey level co-occurrence matrix, a statistical method used to measure the textural

information of images, was also included as a predictor variable. A total of 11 predictor variables were extracted in Sentinel-1 consisting of the bands and grey level co-occurrence matrices that were tabulated in Table 1.

Backscatter Polarization	Description
VV	Vertical transmit-Vertical receive
VH	Vertical transmit-Horizontal receive
VV+VH	Vertical transmit-Vertical receive + Vertical transmit-Horizontal receive
Grey Level Co-Occurrence Matrices (GLCM)	
VV_Mean	Vertical transmit-Vertical receive Mean
VV_Variance	Vertical transmit-Vertical receive Variance
VV_Contrast	Vertical transmit-Vertical receive Contrast
VV_Dissimilarity	Vertical transmit-Vertical receive Dissimilarity
VH_Mean	Vertical transmit-Horizontal receive Mean
VV_Variance	Vertical transmit-Horizontal receive Variance
VV_Contrast	Vertical transmit-Horizontal receive Contrast
VV_Dissimilarity	Vertical transmit-Horizontal receive Dissimilarity

Table 1. Sentinel-1 predictor variables.

The same Sentinel-2 images at level-2A with 13 spectral bands used in the Falcata plantations boundary were utilized. The spectral reflectance of the 20-meter bands was employed as predictors for AGB estimation to match the nominal size of the Sentinel-1 and field plots. Those bands in 10- and 60-meter resolution were resampled to 20-meter to include them as predictors. Furthermore, six vegetation indices and four biophysical variables were generated to test their correlation in AGB. There are 22 predictor variables extracted in Sentinel-2 consisting of the multispectral bands, biophysical variables, and vegetation indices shown in Table 2.

Bands	Description
B1	Coastal Aerosol (443 nm)
B2	Blue (490 nm)
B3	Green (560 nm)
B4	Red (665 nm)
B5	Vegetation Red Edge (705 nm)
B6	Vegetation Red Edge (740 nm)
B7	Vegetation Red Edge (783 nm)
B8	Near Infrared (842 nm)
B8A	Vegetation Red Edge (865 nm)
B9	Water Vapour (945 nm)
B11	Short Wave Infrared (1.610 nm)
B12	Short Wave Infrared (2.190 nm)
Biophysical Variables	
LAI	Leaf Area Index
CAB	Chlorophyll content in the leaf
CW	Water Content
FAPAR	Fraction of Absorbed Photosynthetically Active Radiation
Vegetation Indices	Mathematical Formula

NDVI	(Band 8- Band 4)/ (Band 8+ Band 4)
NDI45	(Band 5- Band 4)/ (Band 5+ Band 4)
IRECI	(Band 7- Band 4)/ (Band 5/ Band 4)
TNDVI	[(Band 8- Band 4)/ (Band 8+ Band 4) + 0.5] / 2
SAVI	(Band 8- Band 4/ Band 8+ Band 4+ 0.5) * 1.5
S2REP	(705 + 35 * ((B4+B7)/ 2) - B5/ (B6-B5))

Table 2. Sentinel-2 predictor variables.

2.3.3 Calculation of Field AGB and Carbon Stock. Based on the field data, the AGB value of each tree was computed using the allometric equation developed by ERDS (2012) for Falcata species adopting Tandug (1986), as indicated in equation (1) (ERDS, 2012). The individual tree AGB values were added together to determine the representative AGB for each plot in tons per acre.

$$Y_f = 10^{[-0.9836 + 1.8036 * \log(D) + 0.8702 * \log_10(H)]}, \quad (1)$$

where Y_f = Fresh aboveground biomass yield of Falcata in kilograms (kg)
 D = Diameter in centimeters (cm)
 H = is the, and the Tree height in meters (m)

The amount of carbon in each tree expressed as tons C per tree is calculated by multiplying the biomass per tree with a conversion factor representing the average carbon content in percent (ERDB, 2008). The total carbon stock of the Falcata plantation is determined using the exact computation on a per hectare basis.

$$C = \%C * B, \quad (2)$$

where C = carbon content by mass
 B = aboveground biomass
 $\%C$ = conversion factor formulated by the ERDB 2008, 48.30% for Falcata trees.

2.3.4 AGB Model Development. Using the center coordinates of collected plots, the pixel values for each variable from both Sentinel-1 and Sentinel-2 were extracted. Pearson correlation coefficient (r) was employed to know the relation between the predictor variables and field AGB. Multiple Linear Regression (MLR) was then used to model AGB from the Sentinel-1 and Sentinel-2 predictor variables. Three models were created, and their accuracy in estimating AGB was tested. Models 1 and 2 represented individual Sentinel-1 and Sentinel-2 models, respectively, whereas Model 3 is a combination of Sentinel-1 and Sentinel-2. The coefficient of the determination, referred to as (R^2), and the Root Mean Square Error (RMSE) were calculated to evaluate the AGB models.

2.4 Estimation and Mapping of Aboveground Biomass and Carbon Stock and Accuracy Assessment

The aboveground biomass of Falcata was estimated based on the model that has the better result in the accuracy assessment. The model in equation form was to produce an image in which the value of each pixel is the estimated aboveground biomass value. The carbon stock value of Falcata was then obtained by multiplying the aboveground biomass value by the conversion factor. The new image derived contains the pixel values of the carbon stock.

The accuracy assessment of the AGB and Carbon Stock Maps created based on the derived model was done using the sixteen (16) validation plots consisting of two plots per Falcata stand age. The R^2 and RMSE between the field measured AGB and

calculated carbon stock with the predicted AGB and carbon stock were calculated. The performance of the derived model in predicting AGB and Carbon stock for the different stand ages of Falcata was also considered and analyzed.

$$RMSE = \sqrt{\frac{\sum_{i=1}^n (\hat{Y}_i - Y_i)^2}{n}}, \quad (3)$$

where \hat{Y}_i and Y_i will represent the field measured and predicted AGB of each plot, respectively, and n will be the number plots.

3. RESULTS AND DISCUSSIONS

3.1 Demarcated Boundary of Falcata Plantations

The demarcated boundary of Falcata plantations in Butuan City is depicted in Figure 2. The total area of Falcata was calculated to be 18,303.52 hectares. The accuracy assessment for the classified image has used 2000 reference points and 1000 reference points for each Falcata and non-Falcata class. The classification result has an overall accuracy of 89.55% (Table 3).

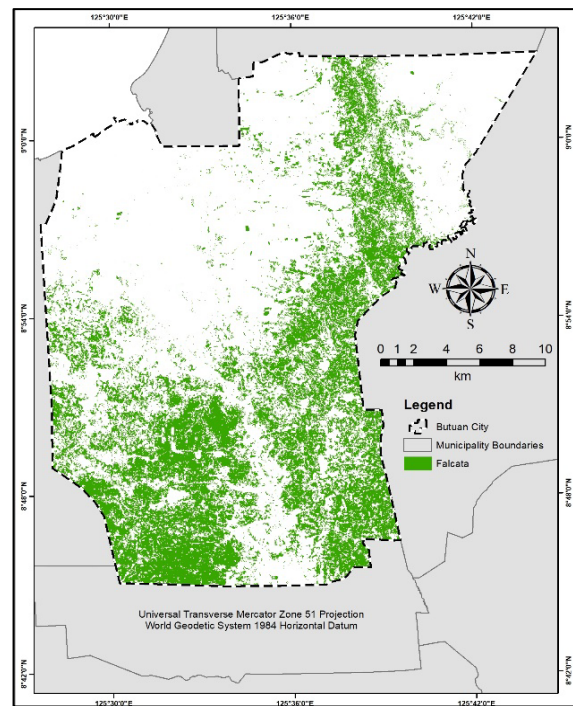


Figure 2. Mapped Falcata Plantations in Butuan City.

		Ground Truth			User's Accuracy (%)
		Falcata	Non-Falcata	Total	
Classifier	Falcata	879	88	967	90.90%
	Non-Falcata	121	912	1033	11.71%
	Total	1000	1000	2000	
	Producer's Accuracy (%)	87.90%	8.80%		
	Overall Accuracy (%)	89.55%			

Table 3. Confusion Matrix of the classification result.

3.2 Correlation of Sentinel-1 variable with Field Measured AGB

Shown in Figure 3 are the correlation coefficients (r) of Sentinel-1 predictor variables ranging from -0.640 to 0.639. Seven (7) out of eleven (11) variables extracted from the Sentinel-1 image showed a significant relationship with the field measured AGB. Only VV backscatter polarization showed a significant correlation at 0.05 level with a correlation value of -0.441. For the grey level co-occurrence matrix variables, VV_Contrast, VV_Dissimilarity, VH_Contrast, and VH_Dissimilarity show significant positive correlation at 0.01 level with a correlation value of 0.614, 0.639, 0.569, and 0.605, respectively. Meanwhile, VV_Mean and VV_Variance show a significant negative correlation at the 0.01 level with a correlation value of -0.640 and -0.638, respectively.

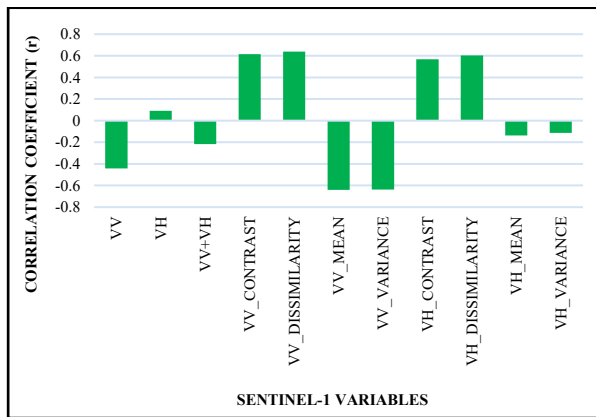


Figure 3. Correlation of Sentinel-1 predictor variables to field measured AGB.

3.3 Correlation of Sentinel-2 variable with Field Measured AGB

The correlation coefficient (r) of Sentinel-2 predictor variables ranged from -0.181 to 0.328 and were graphed in Figure 4. Among the 22 Sentinel-2 predictor variables, only two (2) showed a linear relationship with the field measured AGB; Band 1 and CW. These two variables correlate significantly with the field measured AGB with an r-value of 0.324 and 0.328, respectively.

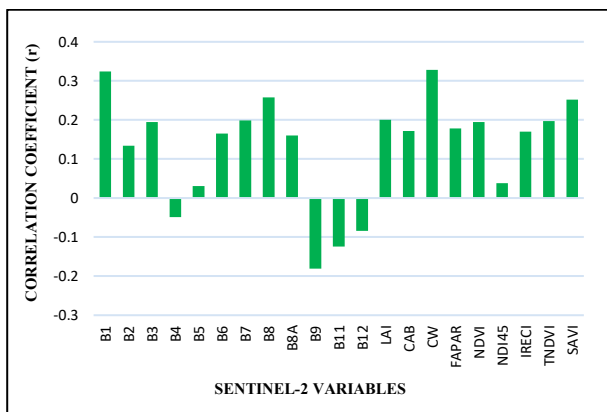


Figure 4. Correlation of Sentinel-2 predictor variables to field measured AGB.

The red-edge bands and the vegetation indices performed poorly, as evidenced by their correlation values. Furthermore,

biophysical variables were extracted to test their potential in predicting Falcata AGB; however, the results were similar to most Sentinel-2 variables, with only CW or water content correlating with AGB. Band 1 and CW are the only predictor variables of Sentinel-2 included in generating the models. Those variables with a significant correlation with the field measured AGB only indicate an existing relationship with the AGB and are thus the only variables considered for AGB model development.

3.4 AGB Model Development

The models generated using the sentinel predictor variables were summarized in Table 4. Model 1 yielded a coefficient of determination (R^2) of 0.610 with an RMSE value of 2.08 ton/pixel. Secondly, Model 2 yielded an R^2 of 0.221 and RMSE of 2.69 ton/pixel. Lastly, Model 3 yielded the highest coefficient r^2 with the value of 0.632 and the lowest RMSE with the value of 1.94 ton/pixel. Model 3, consisting of predictor variables from both Sentinel-1 and Sentinel-2, yielded the highest coefficient of determination and was used in estimating the AGB. This result supported the study of Nuthammachot et al. (2020), which has also reported that the combined use of Sentinel- 1 and 2 predictor variables shows more potential in estimating forest AGB where the model used yielded a coefficient of determination of 0.79. The higher RMSE values could be attributed to the fitness of the model, as statistically expressed by the R^2 of Model 3, which is 0.632.

Models	R^2	RMSE (Ton/Pixel)
Model 1	0.610	2.08
Model 2	0.221	2.69
Model 3	0.632	1.94

Table 4. Root Mean Square Errors (RMSEs) and Coefficient of Determinations (R^2) of each model.

A combination of Sentinel-1 and Sentinel-2 predictor variables was used, and only eight (8) variables were selected to develop the model, and others were excluded. The selected variables were Band 1, VV, VV_Contrast, VV_Mean, VV_Dissimilarity, VV_Variance, VH_Dissimilarity, and VH_Contrast. Although WC also has a significant correlation with AGB, it was excluded in Model 3 as it will generate a model with a higher RMSE value. Generally, grey level co-occurrence matrix variables performed the best and contributed to developing a fitting model for AGB estimation. The study of Kuplich et al. (2003) yielded a higher coefficient of determination when GLCM-derived contrast was utilized. Their study proves that utilization of GLCM derived from Sentinel-1 improves biomass estimation accuracy compared to using the backscatter polarization only (Kuplich et al., 2003). Furthermore, Equation 4 shows the developed equation used to predict AGB.

$$\text{Predicted AGB} = (-0.429 * \text{VV_Variance}) + (23.255 * \text{VV_Mean}) - (1.761 * \text{VV_Dissimilarity}) + (0.310 * \text{VV_Contrast}) + (1.492 * \text{VH_Dissimilarity}) - (0.049 * \text{VH_Contrast}) + (0.122 * \text{VV}) + (0.008 * \text{B1}) - 626.676, \quad (4)$$

3.5 Aboveground Biomass Map Generation

The aboveground biomass map was created using the equation (4). The Falcata boundary area was derived from the demarcated Falcata plantations in Butuan City. Figure 5 illustrates the AGB Map of Falcata plantations in the study area. As seen in the map, the AGB values range from 0 to 38 tons/pixel. Most parts of the Falcata plantations in the study area were bearing the amount of

AGB between 5-8 ton/pixel, and AGB amounting to 15-23 ton/pixel and 24-38 ton/pixel was only minimal.

3.6 Carbon Stock Map Generation

The carbon stock map of Falcata plantations computed from the AGB map depicts Figure 6. This map has a similar trend to AGB. It was derived from the latter. It can be seen that the Carbon Stock value of Falcata in the study area ranges from 0 to 18 tons/pixel. Most of the Falcata plantations in the study area were bearing the amount of Carbon Stock between 2-3 tons/pixel, and Carbon Stock amounting to 7 to 10 tons/pixel and 11 to 18 tons/pixel were only minimal.

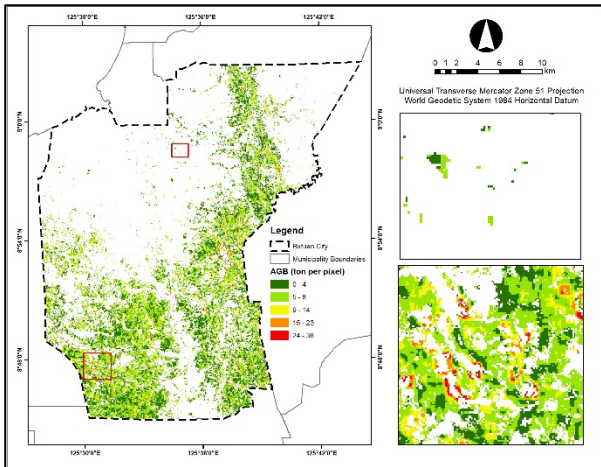


Figure 5. Aboveground Biomass Map of Falcata Plantations in Butuan City.

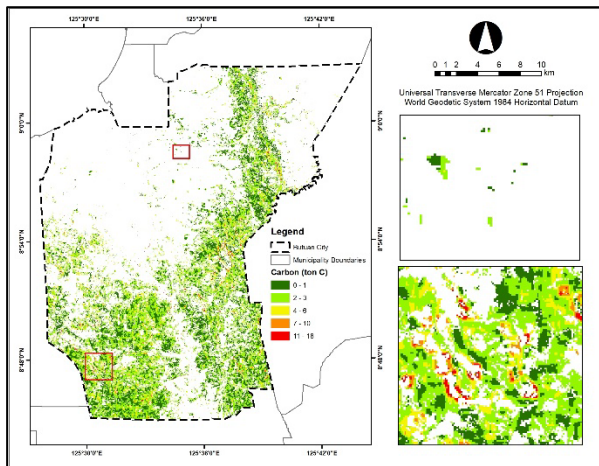


Figure 6. Carbon Stock Map of Falcata Plantations in Butuan City.

3.7 Accuracy assessment of Estimated Aboveground Biomass and Carbon Stock

The scatterplot between field measured and predicted AGB and its coefficient of determination (R^2) of 0.6825 is shown in Figure 7. The garnered R^2 value means that the model has the potential to estimate aboveground biomass. Also, the RMSEs per stand age of the validation plots were tabulated in Table 5. Falcata aging 4-year-old has the lowest RMSE of all the stand ages and 1-year-old with the highest value of RMSE of 0.55 ton/pixel and 2.87 ton/pixel, respectively. This result shows that the final AGB model most accurately estimates the 4-year-old Falcata and least estimates the 1-year-old Falcata. Nevertheless, the overall RMSE

of 1.76 ton/pixel denotes that the final AGB model is moderately good and acceptable in estimating AGB and carbon stock of all Falcata Stand Ages.

The scatterplot of the linear relationship between calculated and predicted Carbon Stock is shown in Figure 8. It shows the relationship between calculated and predicted Carbon Stock with an R^2 of 0.6809. The root mean RMSE per stand age of the plots used in validating Carbon Stock is also shown in Table 5. Falcata, ages 4-year-old, has the lowest RMSE of all the stand ages, followed by Falcata, ages 7, 6, 2, 5, 8, 3, and 1 year old, with the highest RMSE. The Carbon Stock was derived from AGB Map; thus, the value of R^2 generated was nearly equal, and the RMSE had a similar trend to the latter.

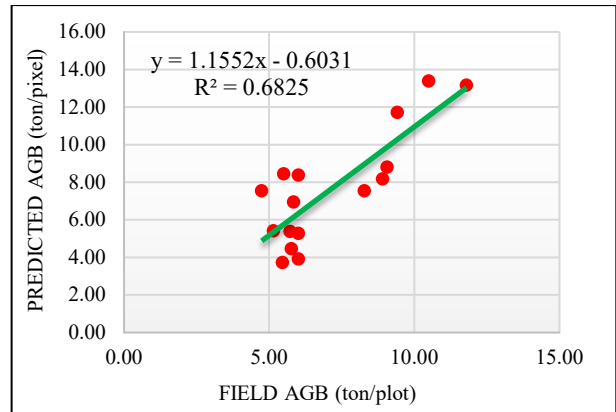


Figure 7. Scatter plot between field AGB and predicted AGB of the validation plots.

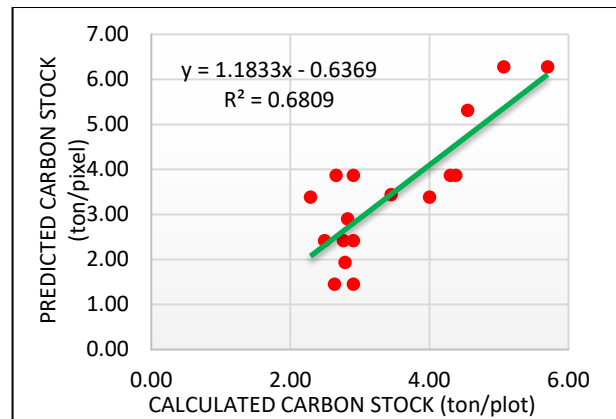


Figure 8. Scatter plot between calculated Carbon Stock and predicted Carbon Stock of the validation plots.

Falcata Stand Age	AGB RMSE (Ton/pixel)	Carbon Stock RMSE (Ton/pixel)
1	2.87	1.15
2	1.24	0.84
3	1.50	1.06
4	0.55	0.48
5	2.33	0.87
6	1.21	0.60
7	0.74	0.56
8	2.26	0.95
Overall RMSE	1.76	0.84

Table 5. RMSEs of AGB and Carbon Stock per Stand Age.

4. CONCLUSIONS AND RECOMMENDATIONS

This study underpins the essence of combining satellite data for a robust and accurate AGB and Carbon Stock Estimation. Model 3, consisting of the combined predictor variables from the two satellite images, has the highest R^2 and lowest RMSE values of 0.632 and 1.94 ton/pixel, respectively. It comprises eight predictor variables from Sentinel-1 and Sentinel-2 images that have a significant relationship with the field AGB and has R^2 values ranging from 0.104 to 0.409, with high correlations observed in GLCM variables. This result shows that Sentinel 1 derived variables show more potential in Falcata AGB estimation than the results achieved with Sentinel 2 extracted variables. Moreover, the final AGB Model was found to perform best in estimating AGB and Carbon Stock of 4-year-old Falcata and performed poorly in 1-year-old Falcata. Nevertheless, its overall R^2 and RMSE have proven that the model is moderately good and acceptable in predicting AGB of all stand ages of Falcata and, indirectly, the carbon stock.

It can also observe that the amount of AGB and Carbon stock can also be attributed to its location. Based on this result, Falcata trees found in remote areas, which are inaccessible and have less human disturbance and other anthropogenic activities, tend to yield higher aboveground biomass and carbon stock than those found near roads built-up areas.

The methodology was applied in a small-scale area like Butuan City. The study still has some limitations and the researchers recommended testing it in larger geographic areas. The Falcata AGB model might be modified in the future using high spatial resolution imagery and different combinations of satellite images. It is also recommended to use the Global Navigation Satellite System (GNSS) to record more accurate coordinates of the plots and the Unmanned Aerial System (UAS) for efficient ground truth data collection. Furthermore, quantifying Falcata belowground biomass and aboveground biomass is recommended to generate a more reliable and precise carbon stock estimation of Falcata Plantations.

REFERENCES

- Bolastig, C., 2019. *Aboveground Biomass Estimation of Mangroves Using Sentinel-1 Images*.
- Chauhan, S. K., Singh, S., Sharma, S., Sharma, R., & Saralch, H. S., 2019. Tree biomass and carbon sequestration in four short rotation tree plantations. *Range Management and Agroforestry*, 40(1), 77–82.
- ERDB., 2008. Biomass and carbon sequestration of forest plantation species in the Philippines. Unpublished terminal report. *Ecosystems Research and Development Bureau, Department of Environment and Natural Resources*.
- ERDS., 2012. Semi-Annual Narrative Accomplishment Report for CY 2012. In *Ecosystems Research and Development Services*.
- IPCC (Intergovernmental Panel on Climate Change)., 1996. *Revised Guidelines*. Cambridge University Press, Cambridge.
- Krisnawati, H., Varis, E., Kallio, M.H., Kanninen, M., 2011. *Paraserianthes falcataria (L.) Nielsen: Ecology, silviculture and productivity. Paraserianthes Falcataria (L.) Nielsen: Ecology, Silviculture and Productivity*.
<https://doi.org/10.17528/cifor/003394>
- Kuplich, T. M., Curran, P. J., & Atkinson, P. M., 2003. Relating SAR image texture and backscatter to tropical forest biomass. *IGARSS 2003. 2003 IEEE International Geoscience and Remote Sensing Symposium. Proceedings (IEEE Cat. No.03CH37477)*, 4, 2872–2874. <https://doi.org/10.1109/IGARSS.2003.1294615>
- Lantican, N. L. and Sy, M., 2020. Estimation of the Carbon Sequestration Rates and Carbon Densities of Forest-tree plantations in Mindanao, Philippines. *Tech. J. Philipp. Ecosyst. Nat. Resour*, vol. 30 (1), pp. 47-65.
- Mauya, E. W., Hansen, E. H., Gobakken, T., Bollandsås, O. M., Malimbwi, R. E., Næsset, E., 2015. Effects of field plot size on prediction accuracy of aboveground biomass in airborne laser scanning-assisted inventories in tropical rain forests of Tanzania. *Carbon Balance and Management*, 10(1), 10. <https://doi.org/10.1186/s13021-015-0021-x>
- Nuthammachot, N., Askar, A., Stratoulis, D., & Wicaksono, P., 2020. Combined use of Sentinel-1 and Sentinel-2 data for improving above-ground biomass estimation. *Geocarto International*, 0, 1–11. <https://doi.org/10.1080/10106049.2020.1726507>
- Powell, S. L., Cohen, W. B., Healey, S. P., Kennedy, R. E., Moisen, G. G., Pierce, K. B., & Ohmann, J. L., 2010. Quantification of live aboveground forest biomass dynamics with Landsat time-series and field inventory data: A comparison of empirical modeling approaches. *Remote Sensing of Environment*, 114(5), 1053–1068. <https://doi.org/10.1016/j.rse.2009.12.018>
- Steiner, M. and Baker, J., 2022. *Measuring Tree Height using a Clinometer*. Csm.
- Stern, N., 2006. Stern Review: the Economics of Climate Change. *HM Treasury, Cambridge University Press, UK*.
- Vashum K. T., Jayakumar S., 2012. Methods to Estimate Above-Ground Biomass and Carbon Stock in Natural Forests - A Review. *Journal of Ecosystem & Ecography*, 02(04). <https://doi.org/10.4172/2157-7625.1000116>